OPEN ACCESS Freely available online

PLoS one

# Visualization of Painful Experiences Believed to Trigger the Activation of Affective and Emotional Brain Regions in Subjects with Low Back Pain

**Kazuhiro Shimo[1], Takefumi Ueno[2], Jarred Younger[3], Makoto Nishihara[1], Shinsuke Inoue[1], Tatsunori Ikemoto[4], Shinichirou Taniguchi[5], Takahiro Ushida[1,5]***

**1** Multidisciplinary Pain Center, Aichi Medical University, Aichi, Japan, **2** Department of Neuropsychiatry, Kyushu University, Fukuoka, Japan, **3** Department of Anesthesia, School of Medicine, Stanford University, Stanford, California, United States of America, **4** NPO Pain Medicine Research Information Center, Kochi, Japan, **5** Department of Orthopaedic Surgery, Kochi Medical School, Kochi, Japan

## Abstract

In the management of clinical low back pain (LBP), actual damage to lower back areas such as muscles, intervertebral discs etc. are normally targeted for therapy. However, LBP may involve not only sensory pain, but also underlying affective pain which may also play an important role overall in painful events. Therefore we hypothesized that visualization of a painful event may trigger painful memories, thus provoking the affective dimension of pain. The present study investigated neural correlates of affect processing in subjects with LBP (n = 11) and subjects without LBP (n = 11) through the use of virtual LBP stimuli. Whole brain functional magnetic resonance imaging (MRI) was performed for all subjects while they were shown a picture of a man carrying luggage in a half-crouching position. All subjects with LBP reported experiencing discomfort and 7 LBP subjects reported experiencing pain. In contrast to subjects without LBP, subjects with LBP displayed activation of the cortical area related to pain and emotions: the insula, supplementary motor area, premotor area, thalamus, pulvinar, posterior cingulate cortex, hippocampus, fusiform, gyrus, and cerebellum. These results suggest that the virtual LBP stimuli caused memory retrieval of unpleasant experiences and therefore may be associated with prolonged chronic LBP conditions.

**Citation:** Shimo K, Ueno T, Younger J, Nishihara M, Inoue S, et al. (2011) Visualization of Painful Experiences Believed to Trigger the Activation of Affective and Emotional Brain Regions in Subjects with Low Back Pain. PLoS ONE 6(11): e26681. doi:10.1371/journal.pone.0026681

**Editor:** Kazutaka Ikeda, Tokyo Metropolitan Institute of Medical Science, Japan

**Received** July 1, 2011; **Accepted** October 2, 2011; **Published** November 2, 2011



**Funding:** This work was supported by a Grant-in-Aid for Scientific Research from the Ministry of Health, Labour, and Welfare. The funders had no role in study design, data collection and analysis, decision to publish, or preparation of the manuscript.

**Competing Interests:** The authors have declared that no competing interests exist.

* E-mail: ushidat-koc@umin.ac.jp

## Introduction

Psychological factors are known to affect the subjective experience of pain. Pain catastrophizing is one such maladaptive response to pain that is characterized by heightened pain intensity [1], increased disability [2]and difficulty disengaging from pain [3]. Recently, functional neuroimaging techniques have been developed that allow the neural correlates of psychological states to be explored. The blood oxygenation level-dependent contrast (BOLD-fMRI) is currently the most popular tool for mapping human brain activity [4]. Pain-related brain activations which could be considered as psychological factors have been reported in various studies. In healthy volunteers, several brain regions, including the primary and secondary somatosensory cortices, insula, anterior cingulate cortex (ACC), thalamus, and motor cortex, respond to real noxious stimuli and are regarded as part of the "pain matrix" [5,6]. However, it is also known that the expectation of pain can evoke brain activation patterns resembling that of a real pain experience [7].

In a previous study [8,9], Ogino reported that the imagination of pain even without physical injury engages the cortical representations of the pain-related neural network. Also, we reported that prior pain experiences can strongly affect pain anticipation and associated brain activations. We have also found that the anticipation of painful stimuli can cause the activation of cortical areas underlying pain-related affect in chronic neuropathic pain patients [10]. Activation in the brain during the visualization of a painful experience was found in the ACC and the medial prefrontalcortex (MPFC), which are regions known to be areas associated with pain and affect processing. Similar activations were found to be correlated with pain catastrophizing in individuals with fibromyalgia [11]. In that study, pain catastrophizing was associated with greater activity in the dorsolateral prefrontal cortex, rostral ACC, and MPFC, regions implicated in pain vigilance, attention and awareness [12,13,14,15]. These results suggest that pain-related neuronal activities might reflect the development and maintenance of chronic pain syndromes.

Low back pain (LBP) is one of the most common chronic pain syndromes. A recent fMRI study in humans reported actual LBP-related cerebral substrates [16]. Abnormal activations were identified in the prefrontal cortex, insula, thalamus, posterior cingulate cortex (PCC), supplementary motor area (SMA), and premotor areas (PMA) – predominantly in the right hemisphere.

**Table 1.** Evaluations of task-related discomfort and pain.

| | LBP group (n = 11) | non-LBP group(n = 11) |
|---|---|---|
| Experiences evoked by tasks | | |
| Discomfort (range) | 3.5 (1–6) | 0 |
| Pain (range) | 2.1 (0–6) | 0 |
| RDQ (mean ± SD) | 3.1±3.1 | 0 |
| ODI (mean ± SD) | 19.8±7.8% | 0 |

RDQ, Roland-Morris Disability Questionnaire; ODI, Oswestry Disability Index 2.0.
doi:10.1371/journal.pone.0026681.t001

We hypothesized that visualization of a painful experience would provoke unpleasant emotions, and these emotions might have a role in the maintenance of chronic pain syndromes. The present study investigated neural correlates of affect processing in subjects with nonspecific LBP and subjects without LBP by using virtual visual stimuli.

## Results

### Self-reported discomfort and pain (Table 1)

All subjects in the LBP group reported discomfort associated with viewing the simulated back pain (mean NRS score, 3.5; range, 1–6). 7 of the 11 subjects in the LBP group described pain associated with the task. However, no subjects in the non-LBP group reported any discomfort or pain resulting from viewing the picture of back pain.

### fMRI results

Compared with the non-LBP group, the LBP group demonstrated significantly more activation in the left fusiform, as well as left inferior temporal gyrus, bilateral precentral gyrus, left middle frontal gyrus, left superior frontal gyrus, bilateral thalamus, bilateral caudate, right insula, left postcentral gyrus, bilateral lingual gyrus, bilateral parahippocampal gyrus, right superior temporal gyrus, left angular gyrus, left superior occipital gyrus, left precuneus, left middle temporal gyrus, left posterior cingulate cortex (PCC), and left cerebellum (Table 2,

**Table 2.** Talairach coordinates and Broadmann's areas for regions of statistically significant activation ($p<0.0005$ at voxel level uncorrected threshold) in response to virtual LBP stimulation (task – control condition).

| Anatomical region | Side | Coordinate | Broadmann area | Z score |
|---|---|---|---|---|
| LBP group as compared to non-LBP group | | | | |
| Fusiform gyrus | Lt | −46, −34, −13 | Area 20 | 4.53 |
| Inferior temporal gyrus | Lt | −57, −43, −15 | Area 37 | 3.60 |
| Precentral gyrus | Lt | −32, 8, 38 | Area 9 | 4.38 |
| | Rt | 28, −24, 56 | Area 4 | 4.03 |
| Middle frontal gyrus | Lt | −46, 20, 43 | Area 8 | 3.68 |
| | | −32, 11, 60 | Area 6 | 3.50 |
| Superior frontal gyrus | Lt | −40, 16, 53 | Area 8 | 3.56 |
| Thalamus | Lt | −24, −25, 7 | - | 4.34 |
| | Rt | 24, −27, 0 | - | 3.40 |
| Caudate | Lt | −28, −32, 13 | - | 3.57 |
| | Rt | 38, −35, −3 | - | 3.91 |
| Insula | Rt | 28, −27, 12 | Area 13 | 4.30 |
| | Rt | 34, −20, 18 | Area 13 | 3.50 |
| Postcentral gyrus | Lt | −8, −55, 64 | Area 7 | 4.07 |
| Lingual gyrus | Rt | 18, −62, 0 | Area 19 | 3.99 |
| | Lt | −6, −72, −5 | Area 18 | 3.81 |
| Parahippocampal gyrus | Lt | −36, −43, 0 | Area 19 | 3.96 |
| | Rt | 32, −53, −4 | Area 19 | 3.91 |
| | Rt | 28, −41, −10 | Area 36 | 3.62 |
| Superior temporal gyrus | Rt | 40, −35, 4 | Area 41 | 3.78 |
| Angular gyrus | Lt | −32, −74, 30 | Area 39 | 3.88 |
| Superior occipital gyrus | Lt | −38, −80, 33 | Area 19 | 3.78 |
| Precuneus | Lt | −42, −72, 35 | Area 19 | 3.42 |
| Middle temporal gyrus | Lt | −60, −35, −5 | Area 21 | 3.62 |
| Posterior cingulate gyrus | Lt | −10, −41, 30 | Area 31 | 3.61 |
| | Lt | −4, −43, 37 | Area 31 | 3.55 |
| Cerebellum | Lt | −24, −30, −20 | - | 3.88 |
| non-LBP group as compared to LBP group | | | | |
| Caudate | Rt | 22, −34, 20 | - | 3.61 |

doi:10.1371/journal.pone.0026681.t002

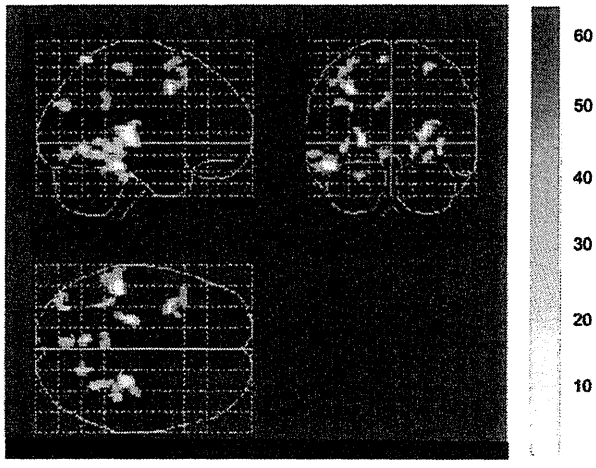


**Figure 1. Areas of cortical activation in the LBP group compared with the non-LBP group in response to virtual LBP stimuli (task – control condition) detected by fMRI($p<0.0005$, Z score>3.4, uncorrected threshold).**
doi:10.1371/journal.pone.0026681.g001

Fig. 1). The reverse contrast showed that the LBP group had lower activations than the non-LBP group in a single cluster in right caudate (Table 2).

In the LBP group, activations related to discomfort were found in the bilateral thalamus, bilateral medial frontal gyrus, right claustrum, left cerebellum (Table 3, Fig. 2). Activations associated with self-reported pain were found in the right thalamus and right lingual gyrus. RDQ scores were associated with activation in the left ACC, and ODI scores were associated with activations in the right insula (Table 3, Fig. 3).

**Table 3.** Cortial areas showing a linear signal increase with the discomfort rating, pain rating, RDQ scores and ODI scores.

| Anatomical region | Side | Coordinate | Broadmann area | Z score |
|---|---|---|---|---|
| Discomfort | | | | |
| Thalamus | Rt | 20, −23, 5 | - | 4.19 |
| | Lt | −4, −17, 3 | - | 3.78 |
| Medial frontal gyrus | Rt | 10, −22, 58 | Area 6 | 3.85 |
| | Lt | −12, −28, 53 | Area 6 | 3.70 |
| | Lt | −50, 1, 28 | Area 6 | 3.38 |
| Claustrum | Rt | 30, 3, 13 | - | 3.75 |
| Cerebellum | Lt | 0, −53, −6 | - | 3.57 |
| Pain | | | | |
| Thalamus | Rt | 20, −31, 7 | - | 4.27 |
| Lingual gyrus | Rt | 8, −86, −11 | Area 18 | 3.62 |
| RDQ | | | | |
| Anterior cingulate gyrus | Lt | −6, 9, 27 | Area 24 | 3.99 |
| ODI | | | | |
| Insula | Rt | 40, −8, −5 | Area 13 | 3.67 |

RDQ, Roland-Morris Disability Questionaire; ODI, Oswestry Disability Index 2.0.
doi:10.1371/journal.pone.0026681.t003

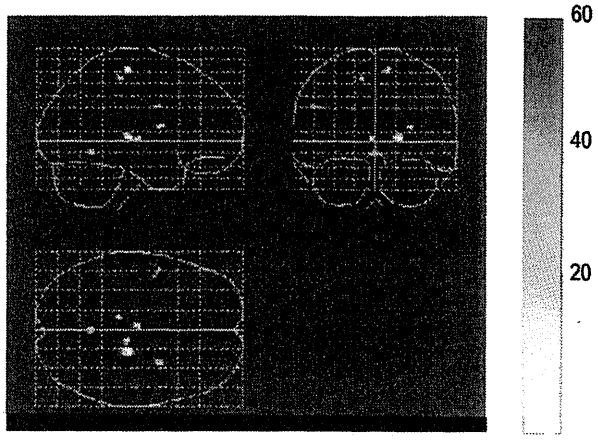


**Figure 2. Areas of cortical activation showing an association with perceived discomfort.**
doi:10.1371/journal.pone.0026681.g002

## Discussion

Our results demonstrate that viewing images of simulated back pain evoke unpleasant feelings, and specific brain activations in individuals with LBP. According to the International Association for the Study of Pain, pain is defined as, "an unpleasant sensory and emotional experience associated with actual or potential tissue damage, or described in terms of such damage". As this definition suggests, both real pain stimuli and virtual pain experiences such as the visual stimuli in our study may play an important role in pain recognition and interpretation in the brain.

Functional MRI results showed that many of the areas described as being part of the "pain matrix" are also active during virtual pain. These results suggest that previous experiences of low back pain can sensitize an individual to pain anticipation. Activation in the insular cortex is associated with pain discrimination [17,18,19]. Additionally, the posterior insular cortex also plays a role in directing appropriate motor behaviors [20]. Furthermore, the insular cortex has projections to the SMA [21,22]. The SMA and PMA are commonly activated by pain [19,23], and usually associated with motor preparation. Activation in those areas might be associated with preparation for protective behavior against pain. In addition, we found virtual LBP stimuli led to increased activation in cerebellum. Activity in the cerebellum is frequently found in pain neuroimaging studies. Cerebellar activation is considered to be primarily associated with motor responses [13]. The need for temporally precise information may also be relevant for brain areas involved in initiating, propagating, and executing defensive motor responses to noxious stimuli [11,13,24,25].

The thalamus and the pulvinar are heavily interconnected with the visual and parietal cortices. Neuroimaging studies suggest responses in the pulvinar have a spatiotopic organization that are modulated by visual attention [26,27,28]. These results suggest that low back pain experiences may make individuals pay more attention to pain-related visual stimuli.

Many reports identify a role of the PCC in negative emotion [29,30,31,32,33,34], visuospatial orientation, and assessment of self-relevant sensation [35]. Exaggerated cerebral activation by pain stimuli may also be associated with pathologic pain states such as allodynia [36,37]. Together with its possible role in inflammatory pain [38], PCC activation could possibly reflect the negative emotion and the pathologic state of pain.

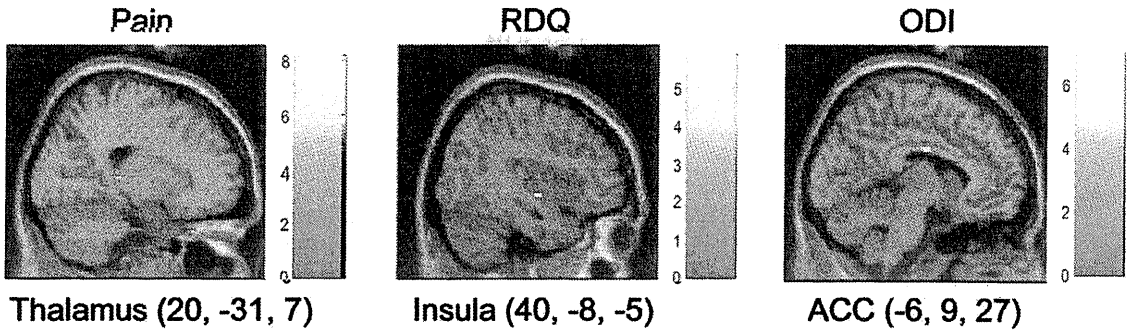


**Figure 3. Sagittal sections showing cortical clusters where activity was linearly correlated with perceived pain, RDQ scores and ODI scores.**
doi:10.1371/journal.pone.0026681.g003

We found other regions with heightened activity in LBP participants, in areas outside of the classic pain matrix. Those regions included the hippocampus, fusiform gyrus and angular gyrus. While not typically considered a nociceptive processing region, activation in the hippocampus has been previously reported to be activated in response to painful heat [14,39] and laser stimulation [40]. The hippocampus has been traditionally associated with recent memory consolidation [41], spatial memory [42], and fear-initiated avoidance behavior [43]. The hippocampus might also play a role in memorizing the pain stimulation and preparing fear-initiated avoidance. The fusiform gyrus is often associated with facial recognition [44]. It is conceivable, therefore, that our visual stimuli (which included a human face) may have been responsible for observed activations in the fusiform gyrus. However, our visual stimuli included a human facewithout any faical expression. This might suggest that the fusiform gyrus plays another important role in the cognitive neuroscience field. The angular gyrus is associated with empathy and 'theory of mind' [45]. Visual stimuli may cause subjects in the LBP group to imagine self pain or feel empathy towards the individual in pain in the picture.

Via parametric analyses in the LBP group, we identified several regional activations that were associated with discomfort rating, pain rating, RDQ scores and ODI scores. The SMA and PMA were related to the discomfort rating. As indicated previously, the SMA and PMA are involved in motor preparation. Activation in those areas might therefore be associated with preparation of protective behaviors against discomfort and pain. Thalamic activation was associated with both discomfort and pain ratings. Greater insula activation was associated with higher ODI scores. The thalamus and insula are considered part of the sensory component of pain processing [46]. But, a recent study suggests that imagining oneself in painful situations is sufficient to trigger some pain sensory regions [47]. The ACC was associated with RDQ scores. The ACC is an important part of affective pain processing [48,49] and can be activated in tasks of pain empathy [47,50,51,52,53,54,55]. It is unknown, therefore, whether the ACC activations, which were observed in the LBP group, were due to imagined self pain, or empathetic pain for the individual in the picture.

In this study, we showed that pain-related visual stimuli can activate several regions of the pain matrix in LBP patients, but not normal volunteers. Moreover, the pain questionnaire scores in the LBP patients were associated with greater activation of pain-processing brain regions. Functional MRI and the virtual visual tasks are non-invasive methods for probing pain-related fear and catastrophizing. These results might be applied to the evaluation of chronic pain syndromes, such as low back pain, in the future.

## Materials and Methods

We recruited subjects with nonspecific LBP (LBP group) (n = 11, 6 male, 5 female, mean age 20.4 years) and subjects without LBP (non-LBP group) (n = 11, 5 male, 6 female, mean age 21.5 years). All participants were right-handed, had no history of cerebrovascular disease, and were free from any medication within 24 hours of the study. Scores for the Roland-Morris Disability Questionnaire (RDQ) and Oswestry Disability Index 2.0 (ODI) were obtained for all participants. Participants in the LBP group reported low back pain, and a RDQ or ODI score greater than zero. Participants in the non-LBP group had never experienced low back pain lasting longer than 1 week, and their RDQ and ODI scores were zero. No participants in either group displayed any evidence of structural abnormality in the lumbar spine on MRI, or any neurologic symptoms. None reported having a history of psychiatric disorders, or currently using any psychoactive medications.

We used virtual LBP stimuli depicting a man who is carrying luggage in a half-crouching position (Fig. 4). This picture represents an action that would likely cause pain in an individual with low back pain, and may therefore cause pain anticipation in the LBP group. Participants were also shown a picture depicting a man standing in front of luggage, providing the baseline stimulation (control condition) (Fig. 4). Participants in the LBP group had painful experiences in the half-crouching posture but did not have any pain in the standing posture. In addition, the participants in the LBP group currently feel little pain in daily life. During the fMRI session, trials were presented in a fixed block design. The distance between the participants' eyes and the screen was 12.5 cm, with a visual angle of 7.4×11.3°. The trials were applied eight times in each series, with each trial presentation lasting 3 seconds. The entire functional experiment lasted 150 seconds (see details of the experimental paradigm in Fig. 4). Self-reported discomfort and pain measures were collected using a numerical rating scale after the experimental session.

Images of the entire brain were acquired using GE SIGNA 3.0 Tesla scanner. Blood oxygenation level-dependent (BOLD) signals were collected with a T2-weighted, multi-slice, gradient echo-planar imaging (EPI) sequence (TE = 35 ms, TR = 3000 ms, flip angle = 90°, slice width = 4 mm, gap = 0 mm, 36 axial slices). Participants were scanned in the supine position, with the head

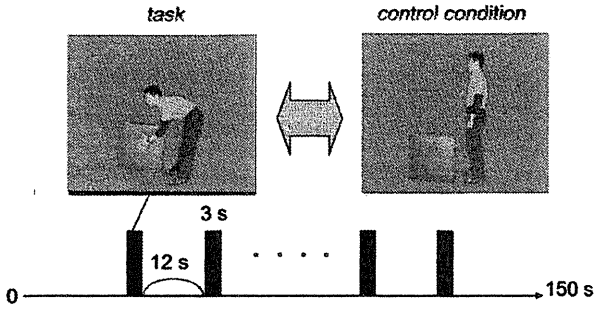


**Figure 4. Experimental design.** Subjects enrolled in the experiment were shown a picture demonstrating a man holding luggage in a half-crouching position (task picture) and a picture demonstrating a man standing in front of luggage, providing the baseline stimulation (control condition picture).
doi:10.1371/journal.pone.0026681.g004

fixed to minimize movement artifact. During the experiment, participants were simply instructed to observe the picture on screen.

The study was approved by the Ethical Committee of Kochi Medical School. All participants were informed of the study purpose beforehand and provided written consent to participate.

Results were analyzed on a Unix workstation using SPM2 (Statistical Parametric Mapping) software; Wellcome Department of Cognitive Neurology, Institute of Neurology, London: http://www.fil.ion.ucl.ac.uk/spm). The acquired images were realigned, spatially normalized to a standard EPI template and finally smoothed with an isotropic Gaussian kernel of 6 mm FWHM (full width at half maximum). Significance was assessed using the box car approach, convolved with the canonical hemodynamic response function. Activation maps represent t-test contrasts between the different experimental conditions. To identify the neural substrates for the virtual pain task, we contrasted the task condition and control condition in the LBP and non-LBP groups. Thresholds for activation were set at $p<0.0005$ for the voxel level of activation, and were further corrected for multiple comparisons at the cluster extent threshold of $p<0.05$. The Talairach atlas was used to anatomically localize foci of significant activation [56]. Brain activation between the LBP group and the non-LBP group was statistically compared to identify the neural processing specific to the LBP group ($p<0.05$, corrected, one-way ANOVA).

For the LBP group only, parametric analyses were also performed to determine associations between brain activity and perceived discomfort, perceived pain, RDQ score and ODI score. Normalized ratings were introduced at the subject level, taking into account only trials from the LBP group.

## Acknowledgments

We would like to thank Mr. Kazuo Morio and Mr. Shin Yaogawa for technical assistance. We are grateful to KMS-TT group for the contributions of general research assistance.

## Author Contributions

Conceived and designed the experiments: KS T. Ushida. Performed the experiments: KS T. Ushida. Analyzed the data: KS T. Ueno JY MN SI T. Ushida. Contributed reagents/materials/analysis tools: TI ST. Wrote the paper: KS T. Ueno JY T. Ushida.

## References

1. Sullivan MJ, Rodgers WM, Kirsch I (2001) Catastrophizing, depression and expectancies for pain and emotional distress. Pain 91: 147–154.
2. Sullivan MJ, Lynch ME, Clark AJ (2005) Dimensions of catastrophic thinking associated with pain experience and disability in patients with neuropathic pain conditions. Pain 113: 310–315.
3. Van Damme S, Crombez G, Eccleston C (2004) Disengagement from pain: the role of catastrophic thinking about pain. Pain 107: 70–76.
4. Apkarian AV, Darbar A, Krauss BR, Gelnar PA, Szeverenyi NM (1999) Differentiating cortical areas related to pain perception from stimulus identification: temporal analysis of fMRI activity. J Neurophysiol 81: 2956–2963.
5. Qiu Y, Noguchi Y, Honda M, Nakata H, Tamura Y, et al. (2006) Brain processing of the signals ascending through unmyelinated C fibers in humans: an event-related functional magnetic resonance imaging study. Cereb Cortex 16: 1289–1295.
6. Wager TD, Rilling JK, Smith EE, Sokolik A, Casey KL, et al. (2004) Placebo-induced changes in FMRI in the anticipation and experience of pain. Science 303: 1162–1167.
7. Koyama T, McHaffie JG, Laurienti PJ, Coghill RC (2005) The subjective experience of pain: where expectations become reality. Proc Natl Acad Sci U S A 102: 12950–12955.
8. Ogino Y, Nemoto H, Inui K, Saito S, Kakigi R, et al. (2007) Inner experience of pain: imagination of pain while viewing images showing painful events forms subjective pain representation in human brain. Cereb Cortex 17: 1139–1146.
9. Ushida T, Ikemoto T, Tanaka S, Shinozaki J, Taniguchi S, et al. (2008) Virtual needle pain stimuli activates cortical representation of emotions in normal volunteers. Neurosci Lett 439: 7–12.
10. Ushida T, Ikemoto T, Taniguchi S, Ishida K, Murata Y, et al. (2005) Virtual pain stimulation of allodynia patients activates cortical representation of pain and emotions: a functional MRI study. Brain Topogr 18: 27–35.
11. Gracely RH, Geisser ME, Giesecke T, Grant MA, Petzke F, et al. (2004) Pain catastrophizing and neural responses to pain among persons with fibromyalgia. Brain 127: 835–843.
12. Bornhovd K, Quante M, Glauche V, Bromm B, Weiller C, et al. (2002) Painful stimuli evoke different stimulus-response functions in the amygdala, prefrontal, insula and somatosensory cortex: a single-trial fMRI study. Brain 125: 1326–1336.
13. Buchel C, Bornhovd K, Quante M, Glauche V, Bromm B, et al. (2002) Dissociable neural responses related to pain intensity, stimulus intensity, and stimulus awareness within the anterior cingulate cortex: a parametric single-trial laser functional magnetic resonance imaging study. J Neurosci 22: 970–976.
14. Derbyshire SW, Jones AK, Gyulai F, Clark S, Townsend D, et al. (1997) Pain processing during three levels of noxious stimulation produces differential patterns of central activity. Pain 73: 431–445.
15. Valet M, Sprenger T, Boecker H, Willoch F, Rummeny E, et al. (2004) Distraction modulates connectivity of the cingulo-frontal cortex and the midbrain during pain–an fMRI analysis. Pain 109: 399–408.
16. Kobayashi Y, Kurata J, Sekiguchi M, Kokubun M, Akaishizawa T, et al. (2009) Augmented cerebral activation by lumbar mechanical stimulus in chronic low back pain patients: an FMRI study. Spine (Phila Pa 1976) 34: 2431–2436.
17. Henderson LA, Gandevia SC, Macefield VG (2007) Somatotopic organization of the processing of muscle and cutaneous pain in the left and right insula cortex: a single-trial fMRI study. Pain 128: 20–30.
18. Korotkov A, Ljubisavljevic M, Thunberg J, Kataeva G, Roudas M, et al. (2002) Changes in human regional cerebral blood flow following hypertonic saline induced experimental muscle pain: a positron emission tomography study. Neurosci Lett 335: 119–123.
19. Svensson P, Minoshima S, Beydoun A, Morrow TJ, Casey KL (1997) Cerebral processing of acute skin and muscle pain in humans. J Neurophysiol 78: 450–460.
20. Berthier M, Starkstein S, Leiguarda R (1988) Asymbolia for pain: a sensory-limbic disconnection syndrome. Ann Neurol 24: 41–49.
21. Augustine JR (1996) Circuitry and functional aspects of the insular lobe in primates including humans. Brain Res Brain Res Rev 22: 229–244.
22. Luppino G, Matelli M, Camarda R, Rizzolatti G (1993) Corticocortical connections of area F3 (SMA-proper) and area F6 (pre-SMA) in the macaque monkey. J Comp Neurol 338: 114–140.
23. Hsieh JC, Stahle-Backdahl M, Hagermark O, Stone-Elander S, Rosenquist G, et al. (1996) Traumatic nociceptive pain activates the hypothalamus and the periaqueductal gray: a positron emission tomography study. Pain 64: 303–314.
24. Peyron R, Kupers R, Jehl JL, Garcia-Larrea L, Convers P, et al. (2007) Central representation of the RIII flexion reflex associated with overt motor reaction: an fMRI study. Neurophysiol Clin 37: 249–259.
25. Sullivan MJ, Thorn B, Haythornthwaite JA, Keefe F, Martin M, et al. (2001) Theoretical perspectives on the relation between catastrophizing and pain. Clin J Pain 17: 52–64.
26. Cotton PL, Smith AT (2007) Contralateral visual hemifield representations in the human pulvinar nucleus. J Neurophysiol 98: 1600–1609.

27. Fischer J, Whitney D (2009) Precise discrimination of object position in the human pulvinar. Hum Brain Mapp 30: 101–111.
28. Smith AT, Cotton PL, Bruno A, Moutsiana C (2009) Dissociating vision and visual attention in the human pulvinar. J Neurophysiol 101: 917–925.
29. Benuzzi F, Lui F, Duzzi D, Nichelli PF, Porro CA (2008) Does it look painful or disgusting? Ask your parietal and cingulate cortex. J Neurosci 28: 923–931.
30. Britton JC, Phan KL, Taylor SF, Welsh RC, Berridge KC, et al. (2006) Neural correlates of social and nonsocial emotions: An fMRI study. Neuroimage 31: 397–409.
31. Maddock RJ, Garrett AS, Buonocore MH (2003) Posterior cingulate cortex activation by emotional words: fMRI evidence from a valence decision task. Hum Brain Mapp 18: 30–41.
32. Mantani T, Okamoto Y, Shirao N, Okada G, Yamawaki S (2005) Reduced activation of posterior cingulate cortex during imagery in subjects with high degrees of alexithymia: a functional magnetic resonance imaging study. Biol Psychiatry 57: 982–990.
33. Sander K, Frome Y, Scheich H (2007) FMRI activations of amygdala, cingulate cortex, and auditory cortex by infant laughing and crying. Hum Brain Mapp 28: 1007–1022.
34. Sinha R, Lacadie C, Skudlarski P, Wexler BE (2004) Neural circuits underlying emotional distress in humans. Ann N Y Acad Sci 1032: 254–257.
35. Vogt BA (2005) Pain and emotion interactions in subregions of the cingulate gyrus. Nat Rev Neurosci 6: 533–544.
36. Freund W, Wunderlich AP, Stuber G, Mayer F, Steffen P, et al. (2010) Different activation of opercular and posterior cingulate cortex (PCC) in patients with complex regional pain syndrome (CRPS I) compared with healthy controls during perception of electrically induced pain: a functional MRI study. Clin J Pain 26: 339–347.
37. Lorenz J, Cross DJ, Minoshima S, Morrow TJ, Paulson PE, et al. (2002) A unique representation of heat allodynia in the human brain. Neuron 35: 383–393.
38. Ruehle BS, Handwerker HO, Lennerz JK, Ringler R, Forster C (2006) Brain activation during input from mechanoinsensitive versus polymodal C-nociceptors. J Neurosci 26: 5492–5499.
39. Ploghaus A, Narain C, Beckmann CF, Clare S, Bantick S, et al. (2001) Exacerbation of pain by anxiety is associated with activity in a hippocampal network. J Neurosci 21: 9896–9903.
40. Bingel U, Quante M, Knab R, Bromm B, Weiller C, et al. (2002) Subcortical structures involved in pain processing: evidence from single-trial fMRI. Pain 99: 313–321.
41. Alvarez P, Squire LR (1994) Memory consolidation and the medial temporal lobe: a simple network model. Proc Natl Acad Sci U S A 91: 7041–7045.
42. Clark RE, Broadbent NJ, Squire LR (2007) The hippocampus and spatial memory: findings with a novel modification of the water maze. J Neurosci 27: 6647–6654.
43. Hollup SA, Kjelstrup KG, Hoff J, Moser MB, Moser EI (2001) Impaired recognition of the goal location during spatial navigation in rats with hippocampal lesions. J Neurosci 21: 4505–4513.
44. Radua J, Phillips ML, Russell T, Lawrence N, Marshall N, et al. (2010) Neural response to specific components of fearful faces in healthy and schizophrenic adults. Neuroimage 49: 939–946.
45. Vollm BA, Taylor AN, Richardson P, Corcoran R, Stirling J, et al. (2006) Neuronal correlates of theory of mind and empathy: a functional magnetic resonance imaging study in a nonverbal task. Neuroimage 29: 90–98.
46. Bushnell MC, Duncan GH, Hofbauer RK, Ha B, Chen JI, et al. (1999) Pain perception: is there a role for primary somatosensory cortex? Proc Natl Acad Sci U S A 96: 7705–7709.
47. Jackson PL, Brunet E, Meltzoff AN, Decety J (2006) Empathy examined through the neural mechanisms involved in imagining how I feel versus how you feel pain. Neuropsychologia 44: 752–761.
48. Apkarian AV, Bushnell MC, Treede RD, Zubieta JK (2005) Human brain mechanisms of pain perception and regulation in health and disease. Eur J Pain 9: 463–484.
49. Davis KD, Taylor KS, Hutchison WD, Dostrovsky JO, McAndrews MP, et al. (2005) Human anterior cingulate cortex neurons encode cognitive and emotional demands. J Neurosci 25: 8402–8406.
50. Botvinick M, Jha AP, Bylsma LM, Fabian SA, Solomon PE, et al. (2005) Viewing facial expressions of pain engages cortical areas involved in the direct experience of pain. Neuroimage 25: 312–319.
51. Gu X, Han S (2007) Attention and reality constraints on the neural processes of empathy for pain. Neuroimage 36: 256–267.
52. Jackson PL, Meltzoff AN, Decety J (2005) How do we perceive the pain of others? A window into the neural processes involved in empathy. Neuroimage 24: 771–779.
53. Lamm C, Batson CD, Decety J (2007) The neural substrate of human empathy: effects of perspective-taking and cognitive appraisal. J Cogn Neurosci 19: 42–58.
54. Morrison I, Lloyd D, di Pellegrino G, Roberts N (2004) Vicarious responses to pain in anterior cingulate cortex: is empathy a multisensory issue? Cogn Affect Behav Neurosci 4: 270–278.
55. Singer T, Seymour B, O'Doherty J, Kaube H, Dolan RJ, et al. (2004) Empathy for pain involves the affective but not sensory components of pain. Science 303: 1157–1162.
56. Talairach J, Tournoux P (1988) Co-planar Stereotaxic Atlas of the Human Brain. New York: Thime Medical Publishers. 122 p.

Mod Rheumatol (2012) 22:40–44
DOI 10.1007/s10165-011-0462-3

ORIGINAL ARTICLE

# The Japanese version of the 2010 American College of Rheumatology Preliminary Diagnostic Criteria for Fibromyalgia and the Fibromyalgia Symptom Scale: reliability and validity

**Chie Usui · Kotaro Hatta · Satoko Aratani · Naoko Yagishita · Kenya Nishioka · Teruhisa Kanazawa · Kenji Ito · Yoshihisa Yamano · Hiroyuki Nakamura · Toshihiro Nakajima · Kusuki Nishioka**

Received: 28 February 2011 / Accepted: 20 April 2011 / Published online: 10 May 2011


**Abstract** The aim of this study was to investigate the reliability and the validity of the Japanese version of the 2010 American College of Rheumatology Preliminary Diagnostic Criteria for Fibromyalgia (ACR 2010-J), and its quantification scale, the Fibromyalgia Symptom Scale (FS-J). In this study, we divided patients with chronic pain without psychiatric disorders other than depression into two groups according to the 1990 ACR Diagnostic Criteria for Fibromyalgia, a fibromyalgia group and a non-fibromyalgia group (rheumatoid arthritis, osteoarthritis, and gout). Patients in both groups were assessed using the ACR 2010-J and FS-J. Seventy-seven of 94 (82%) patients in the fibromyalgia group met the ACR 2010-J, whereas 9% (4/43) of the non-fibromyalgia group did so, with a sensitivity of 82%, specificity of 91%, positive predictive value of 95%, negative predictive value of 70%, and positive likelihood ratio of 8.8. Mean total scores on the FS-J significantly differentiated the fibromyalgia from the non-fibromyalgia group. The scale had high inter-rater reliability and high internal consistency. With a cutoff score of 10, the positive likelihood ratio was 10.1. Our findings indicate that the ACR 2010-J and FS-J have high reliability and validity, and are useful for assessing fibromyalgia in Japanese populations with chronic pain. As regards the positive likelihood ratio, that of the FS-J might be suitable as a positive test.

**Keywords** ACR Preliminary Diagnostic Criteria for Fibromyalgia 2010 · Diagnostic criteria · Fibromyalgia · Symptom scale

C. Usui (✉) · K. Hatta
Department of Psychiatry, Juntendo University School of Medicine, Juntendo University Nerima Hospital, 3-1-10 Takanodai, Nerima-ku, Tokyo 177-8521, Japan
e-mail: chiec@juntendo.ac.jp

S. Aratani · T. Nakajima · K. Nishioka
Institute of Innovative Medical Science and Education, Tokyo Medical University, 6-1-1 Shinjuku, Shinjuku-ku, Tokyo 160-8402, Japan

N. Yagishita · Y. Yamano
Institute of Medical Science, St. Marianna University School of Medicine, 2-16-1 Sugo, Miyame-ku, Kawasaki, Kanagawa 216-8511, Japan

K. Nishioka
Department of Neurology, Juntendo University School of Medicine, 2-1-1 Hongo, Bunkyo-ku, Tokyo 113-8421, Japan

T. Kanazawa
Department of Rheumatology, Tokyo Medical University Ibaraki Medical Center, 3-20-1 Chuo, Ami-cho, Inashiki-gun, Ibaraki 300-0395, Japan

K. Ito
Department of Rheumatology, National Center for Global Health and Medicine, 1-21-1 Toyama, Shinjuku-ku, Tokyo 162-8655, Japan

H. Nakamura
Department of Environmental and Preventive Medicine, Graduate School of Medical Science, Kanazawa University, Kakuma-cho, Kanazawa, Kanazawa 920-1192, Japan

## Introduction

Fibromyalgia is characterized by widespread chronic musculoskeletal pain, fatigue, poor sleep, frequent psychological difficulties, and multiple tender points on physical examination [1, 2]. In 1990, the American College of Rheumatology (ACR) presented fibromyalgia criteria (ACR 1990) that required tenderness on pressure (tender points) in at least 11 of 18 specified sites and the presence

of widespread pain for diagnosis [1]. Widespread pain was defined as axial pain, both left- and right-sided and with upper and lower segment pain. However, the ACR 1990 had the serious problem of little variation in symptoms. To improve this shortcoming, new clinical criteria, which integrate variations in symptoms with a severity scale (2010 ACR Preliminary Diagnostic Criteria for Fibromyalgia, ACR 2010), have been presented [3]. The criteria consist of the widespread pain index (WPI) and the Symptom Severity Scale (SS) (Table 1).

Recently, a 0–31 Fibromyalgia Symptom Scale (Fibromyalgia Symptom Scale, FS), created by adding the WPI to the modified SS scale, has also been proposed, which will allow the use of these scales in epidemiologic and clinical studies without the requirement for an examiner; further, the FS can also be used to determine widespread pain according to the 1990 ACR classification criteria [4]. The consecutive scoring is easy to use and easy to understand.

The aim of this study was to investigate the reliability and validity of both the Japanese version of the ACR 2010 (ACR 2010-J) and the Japanese version of the FS (FS-J).

## Subjects and methods

An experienced rheumatologist and a psychiatrist had translated the ACR 2010 into Japanese with the author's

**Table 1** Fibromyalgia diagnostic criteria 2010

Criteria

A patient satisfies diagnostic criteria for fibromyalgia if the following 3 conditions are met:

(1) Widespread pain index (WPI) ≥7 and symptom severity (SS) scale score ≥5 or WPI 3–6 and SS scale score ≥9

(2) Symptoms have been present at a similar level for at least 3 months

(3) The patient does not have a disorder that would otherwise explain the pain

Ascertainment

(1) WPI: note the number of areas in which the patient has had pain over the last week. In how many areas has the patient had pain? Score will be between 0 and 19

| | | | |
|---|---|---|---|
| Shoulder girdle, left | Hip (buttock, trochanter), left | Jaw, left | Upper back |
| Shoulder girdle, right | Hip (buttock, trochanter), right | Jaw, right | Lower back |
| Upper arm, left | Upper leg, left | Chest | Neck |
| Upper arm, right | Upper leg, right | Abdomen | |
| Lower arm, left | Lower leg, left | | |
| Lower arm, right | Lower leg, right | | |

(2) SS scale score:

Fatigue

Waking unrefreshed

Cognitive symptoms

For each of the 3 items in the SS scale score, above, indicate the level of severity of the symptoms over the past week, using the following scale:

0 = no problem

1 = slight or mild problems, generally mild or intermittent

2 = moderate, considerable problems, often present and/or at a moderate level

3 = severe: pervasive, continuous, life-disturbing problems

Considering somatic symptoms in general, indicate whether the patient has:[a]

0 = no symptoms

1 = few symptoms

2 = a moderate number of symptoms

3 = a large number of symptoms

The SS scale score is the sum of the severity of the 3 items –fatigue, waking unrefreshed, cognitive symptoms–plus the extent (severity) of somatic symptoms in general. The final score is between 0 and 12

[a] Somatic symptoms that might be considered: muscle pain, irritable bowel syndrome, fatigue/tiredness, thinking of or remembering problems, muscle weakness, headache, pain/cramps in the abdomen, numbness/tingling, dizziness, insomnia, depression, constipation, pain in the upper abdomen, nausea, nervousness, chest pain, blurred vision, fever, diarrhea, dry mouth, itching, wheezing, Raynaud's phenomenon, hives/welts, ringing in ears, vomiting, heartburn, oral ulcers, loss of/change in taste, seizures, dry eyes, shortness of breath, loss of appetite, rash, sun sensitivity, hearing difficulties, easy bruising, hair loss, frequent urination, painful urination, and bladder spasms

permission and produced forward- and back-translations to create the ACR-J.

We recruited fibromyalgia patients who met the previous criteria for diagnosis (ACR 1990) and were without psychiatric disorders according to the Diagnostic and Statistical Manual of Mental Disorders (DSM-IV) [5]. The patients were recruited at a clinic specialized for fibromyalgia, the Kasumigaseki Urban Clinic, in Tokyo, Japan, between August 1, 2010 and October 31, 2010. During the study period, other patients with diseases associated with chronic pain, such as rheumatoid arthritis (RA), osteoarthritis (OA), and gout, who had not been diagnosed previously with fibromyalgia were recruited as control patients. The diagnoses of RA, OA, and gout were made according to the 2010 RA classification criteria [4]; the ACR criteria for the classification and reporting of OA of the hand, hip, and knee [6–8]; and the 1977 criteria for the classification of the acute arthritis of primary gout [9]. An experienced rheumatologist and an experienced psychiatrist familiar with fibromyalgia assessed these patients. This study was approved by the Institutional Review Board of Kasumigaseki Urban Clinic.

After obtaining informed consent from the study participants, the rheumatologist rated patients with the 2010 ACR-J. In order to assess inter-rater reliability, another rater independently rated a subset of the same subjects ($N = 19$) while blind to the diagnoses and scores of the other rater. The raters in this study were already fully trained in the use of the scale and quite experienced in the use of it. We therefore decided that only a small subsample was needed to reevaluate consistency across raters.

## Statistics

Data were analyzed using SPSS 17.0-J software (SPSS, Chicago, IL, USA). Differences among groups in demographic and clinical characteristics were calculated with the unpaired *t*-test. If data were not sampled from Gaussian distributions, a non-parametric test (Mann–Whitney *U*-test) was used. To compare categorical data, we used Fisher's exact test. To control for the effect of age on the percentage of patients meeting the new fibromyalgia criteria, the patients were divided into three age categories, i.e., 20–39, 40–59, and ≥60 years. There was no patient <20 years of age, and there were only 2 fibromyalgia patients and 3 non-fibromyalgia patients aged 80 years or older. The Mantel–Haenszel method was used to test the difference in the percentages of patients meeting the new fibromyalgia criteria between the two groups. Also, to control for the effect of age on the score on the FS, one-way analysis of covariance was used. The internal consistency for the ACR 2010-J was calculated with Cronbach's $\alpha$. Inter-rater reliability was measured with the intra-class correlation coefficient (ICC) for pairs of independent raters. Cutoff scores for the FS-J were determined using receiver-operator characteristic (ROC) analyses to determine acceptable levels of sensitivity and specificity when comparing the fibromyalgia group with all non-fibromyalgia subjects. The positive predictive value (PPV), negative predictive value (NPV), and positive likelihood ratio (sensitivity/1-specificity) were also calculated. All statistical tests were two-tailed. Statistical significance was set at $p < 0.05$.

## Results

A total of 94 patients meeting the ACR 1990 (the fibromyalgia group) and a total of 43 non-fibromyalgia patients (RA patients, 29; OA patients, 9; gout patients, 5 – the non-fibromyalgia group) were enrolled. Demographic and clinical characteristics of the groups are shown in Table 2. Seventy-seven of 94 (82%) patients in the fibromyalgia group met the ACR 2010-J, whereas 9% of the non-fibromyalgia group did so, including 14% of the RA patients, 0% of the OA patients, and 0% of the gout patients. The percentage of patients meeting the new fibromyalgia criteria in the fibromyalgia group was significantly higher than that of the non-fibromyalgia group after adjusting for age (estimated odds ratio 0.042; $p < 0.0001$, Table 2). The sensitivity, specificity, PPV, NPV, and positive likelihood ratio for comparison of the fibromyalgia group with all non-fibromyalgia subjects were 82, 91, 95, 70%, and 8.8, respectively. The ICC between the two independent raters was very high for the ACR 2010-J, at 0.877.

The mean score (SD) of the FS-J in the fibromyalgia group was 18.0 (5.8), while that in the non-fibromyalgia group was 4.9 (4.4). The mean score on the FS in the fibromyalgia group was significantly higher than that of the non-fibromyalgia group after adjusting for age ($F = 105.6$, $p < 0.0001$, Table 2). Internal consistency was high, with a Cronbach's $\alpha$ coefficient for the FS-J (WPI + SS) of 0.747. The ICC between the two independent raters was very high for the FS-J, at 0.994. ROC analyses were performed for the FS-J, comparing the fibromyalgia group to the non-fibromyalgia group. Table 3 shows the sensitivity, specificity, PPV, NPV, and positive likelihood ratio values for ROC analysis at various cutoff scores for the FS-J. Compared with the non-fibromyalgia group, the best cutoff score for the FS-J was 10, resulting in 94% sensitivity, 91% specificity, 96% PPV, 87% NPV, and a positive likelihood ratio of 10.1.

**Table 2** Demographic and clinical characteristics of the fibromyalgia group and non-fibromyalgia group

| Group | Fibromyalgia ($N = 94$) | Non-fibromyalgia ($N = 43$) | | | $p$ |
|---|---|---|---|---|---|
| | | RA ($N = 29$) | OA ($N = 9$) | Gout ($N = 5$) | |
| Mean age, years (SD) | 48.8 (13.3) | 63.0 (12.8) | | | <0.0001 |
| | | 59.9 (13.7) | 70.3 (10.1) | 67.7 (5.1) | |
| Sex, female, *N* (%) | 85 (90) | 33 (77) | | | 0.06 |
| | | 24 (83) | 9 (100) | 0 (0) | |
| Patients meeting the new fibromyalgia criteria[a] *N* (%) | 77 (82) | 4 (9) | | | <0.0001 |
| | | 4 (14) | 0 (0) | 0 (0) | |
| Fibromyalgia Symptom Scale[b] mean score (SD) | 18.0 (5.8) | | 4.9 (4.4) | | <0.0001 |
| | | 5.2 (5.0) | 5.4 (2.2) | 2 (1.9) | |

*RA* rheumatoid arthritis, *OA* osteoarthritis

[a] The 2010 American College of Rheumatology (ACR) Preliminary Diagnostic Criteria for Fibromyalgia

[b] The 2010 ACR Preliminary Diagnostic Criteria for Fibromyalgia consist of the widespread pain index (WPI) and Symptom Severity Scale (SS). The score on the Fibromyalgia Symptom Scale is the total of the WPI and the SS

**Table 3** Sensitivity and specificity of the Fibromyalgia Symptom Scale, based on receiver operating characteristics (ROC) analysis; the fibromyalgia group versus non-fibromyalgia (RA, OA, and gout) group

| Cutoff score | Sensitivity (%) | Specificity (%) | PPV (%) | NPV (%) | Positive likelihood ratio |
|---|---|---|---|---|---|
| 9 | 96 | 86 | 94 | 90 | 6.9 |
| 10 | 94 | 91 | 96 | 87 | 10.1 |
| 11 | 91 | 91 | 96 | 83 | 9.8 |
| 13 | 83 | 91 | 95 | 71 | 8.9 |

*PPV* positive predictive value, *NPV* negative predictive value

## Discussion

This is the first study to validate the ACR 2010-J. The present results, showing very high ICC and high sensitivity, specificity, PPV, NPV, and positive likelihood ratio, indicate that the ACR 2010-J has high reliability and validity, and is useful for assessing fibromyalgia among Japanese chronic pain populations.

Furthermore, the present results showed that the Japanese version of the FS (FS-J), the quantification scale of the ACR 2010-J, also exhibited a high degree of internal consistency, very high ICC, and high sensitivity, specificity, PPV, NPV, and positive likelihood ratio, indicating that the FS-J also has high reliability and validity and is useful for assessing fibromyalgia among Japanese chronic pain populations. In the present study, the best cutoff score was 10, while in a previous study it was found to be 13 [10].

One explanation for the difference in the cutoff scores is in patient characteristics. In the present study, comorbid psychiatric disorders were excluded, while in the previous study they were not. Patients with major depressive disorder, panic disorder, or anxiety disorder usually have somatic symptoms similar to those of the ACR 2010, and comorbidity of major depressive disorder, panic disorder, or anxiety disorder is not rare [11]. Therefore, the population in the previous study [10] may have been modified by the comorbid psychiatric disorders. Thus, the cutoff score of 10 in the present study may more specifically reflect fibromyalgia itself compared with the cutoff score of 13 in the previous study. Another possible explanation for the difference in cutoff scores between that study and ours could be cross-cultural differences in expression or the rating of symptoms.

We found that the positive likelihood ratio of the ACR 2010-J was below 10, while that of the FS-J with a cutoff score of 10 was above 10. Therefore, as regards the positive likelihood ratio, that of the FS-J might be suitable for a positive test.

The strength of the present study is that the findings represent real clinical practice in Japan, since the study was performed in a clinic specialized for fibromyalgia which is visited by the largest number of fibromyalgia patients in Japan. A limitation of this study is that the findings may not be applicable to all patients, since fibromyalgia patients with other musculoskeletal diseases, such as spondylitis, were not included in it. Further studies with patients from

other countries or those of other ethnicities will be needed to determine cross-cultural or ethnic differences in expression or the rating of symptoms.

**Acknowledgments** This work was supported in part by grants from the Arthritis Foundation of the Ministry of Health, Welfare, and Labour of Japan and the Japan Rheumatology Foundation and by a Grant-in-Aid for Young Scientists B (22791142) from the Japan Society for the Promotion of Science.

**Conflict of interest** None.

## References

1. Wolfe F, Smythe HA, Yunus MB, Bennett RM, Bombardier C, Goldenberg DL, et al. The American College of Rheumatology 1990 Criteria for the Classification of Fibromyalgia. Report of the Multicenter Criteria Committee. Arthritis Rheum. 1990;33(2): 160–72.
2. Wolfe F, Ross K, Anderson J, Russell IJ, Hebert L. The prevalence and characteristics of fibromyalgia in the general population. Arthritis Rheum. 1995;38(1):19–28.
3. Wolfe F, Clauw DJ, Fitzcharles MA, Goldenberg DL, Katz RS, Mease P, et al. The American College of Rheumatology preliminary diagnostic criteria for fibromyalgia and measurement of symptom severity. Arthritis Care Res. 2010;62(5):600–10.
4. American Psychiatric Association. Diagnostic and Statistical Manual of Mental Disorders. 4th ed. Washington D.C.: American Psychiatric Association; 1996.
5. Aletaha D, Neogi T, Silman AJ, Funovits J, Felson DT, Bingham CO 3rd, et al. Rheumatoid arthritis classification criteria: an American College of Rheumatology/European League Against Rheumatism collaborative initiative. Ann Rheum Dis. 2010; 69(9):1580–8.
6. Altman R, Alarcon G, Appelrouth D, Bloch D, Borenstein D, Brandt K, et al. The American College of Rheumatology criteria for the classification and reporting of osteoarthritis of the hip. Arthritis Rheum. 1991;34(5):505–14.
7. Altman R, Alarcon G, Appelrouth D, Bloch D, Borenstein D, Brandt K, et al. The American College of Rheumatology criteria for the classification and reporting of osteoarthritis of the hand. Arthritis Rheum. 1990;33(11):1601–10.
8. Altman R, Asch E, Bloch D, Bole G, Borenstein D, Brandt K, et al. Development of criteria for the classification and reporting of osteoarthritis. Classification of osteoarthritis of the knee. Diagnostic and Therapeutic Criteria Committee of the American Rheumatism Association. Arthritis Rheum. 1986;29(8):1039–49.
9. Wallace SL, Robinson H, Masi AT, Decker JL, McCarty DJ, Yu TF. Preliminary criteria for the classification of the acute arthritis of primary gout. Arthritis Rheum. 1977;20(3):895–900.
10. Wolfe F, Clauw DJ, Fitzcharles MA, Goldenberg DL, Hauser W, Katz RS, et al. Fibromyalgia Criteria and Severity Scale for Clinical and Epidemiological Studies: a modification of the ACR Preliminary Diagnostic Criteria for Fibromyalgia. In: ACR2010: Atlanta; 2010. p. 100.
11. Arnold LM, Hudson JI, Keck PE, Auchenbach MB, Javaras KN, Hess EV. Comorbidity of fibromyalgia and psychiatric disorders. J Clin Psychiatry. 2006;67(8):1219–25.

J Orthop Sci (2011) 16:710–718
DOI 10.1007/s00776-011-0149-9

ORIGINAL ARTICLE

# Three-dimensional in vivo motion analysis of normal knees using single-plane fluoroscopy

**Osamu Tanifuji · Takashi Sato · Koichi Kobayashi · Tomoharu Mochizuki · Yoshio Koga · Hiroshi Yamagiwa · Go Omori · Naoto Endo**

Received: 8 February 2011 / Accepted: 10 August 2011 / Published online: 4 September 2011


**Abstract**
*Background* Analysis of the movement of anatomically defined reference axes at the femoral condyles relative to the tibia is appropriate for evaluating knee kinematics. However, such parameters have been previously employed only in studies utilizing stop-motion techniques. The purpose of this study was to evaluate in vivo dynamic kinematics for full range of motion in normal knees using the three-dimensional to two-dimensional registration technique and to compare them with previously reported normal knee kinematics obtained via stop-motion techniques.
*Methods* Dynamic motion of the right knee was analyzed in 20 healthy volunteers (10 female, 10 male; mean age 37.2 years). Knee motion was observed when subjects squatted from standing with the knee fully extended to maximum flexion. We determined the following parameters: (1) changes to angles of the geometric center axis (GCA) on the tibial axial plane (rotation angle); (2) anteroposterior translations of the medial and lateral ends of the GCA; and (3) motion patterns in each phase during knee flexion.
*Results* All subjects exhibited femoral external rotation (26.1°) relative to the tibia throughout knee flexion. The medial femoral condyle demonstrated anterior translation (5.5 mm) from full extension to 100° flexion, and demonstrated posterior translation (3.9 mm) after 100°, while the lateral femoral condyle demonstrated consistent posterior translation (15.6 mm) throughout knee flexion. All subjects showed medial pivot motion from full extension to nearly 120° flexion. From 120° flexion, bicondylar rollback motion was observed.
*Discussion* Although the behavior of the medial femoral condyle in our analysis differed somewhat from that seen in previous cadaver studies, the results obtained using dynamic analysis were generally equivalent to those obtained in previous studies employing stop-motion techniques. These results provide control data for future dynamic kinematic analyses of pathological knees.

O. Tanifuji · T. Sato (✉) · T. Mochizuki · Y. Koga
Department of Orthopaedic Surgery, Niigata Medical Center, 3-27-11 Kobari, Nishi-ku, Niigata, Niigata 950-2022, Japan
e-mail: taku409@skyblue.ocn.ne.jp

O. Tanifuji · H. Yamagiwa · N. Endo
Division of Orthopaedic Surgery, Department of Regenerative and Transplant Medicine, Niigata University Graduate School of Medicine and Dental Science, Niigata, Japan

K. Kobayashi
Department of Health Sciences, Niigata University School of Medicine, Niigata, Japan

G. Omori
Center for Transdisciplinary Research, Institute for Research Promotion, Niigata University, Niigata, Japan

## Introduction

Motion analyses of normal knees provide references for the analysis of pathologic knees, as in cases of osteoarthritis or ligament injury, or in the design of total knee prostheses. To describe normal knee motion, methods employing anatomically defined axes at the femoral condyles have been utilized in many studies [1–11]. Asano et al. [1] reported on the motion of the medial and lateral femoral condyles relative to the tibia using the geometric center axis (GCA), defined as the segment connecting the centers of spheres representing the femoral posterior condyles,

while Iwaki et al. [2] and Pinskerova et al. [3] also reported tibiofemoral movement using the medial and lateral flexion facet centers (FFC), represented by centers of circles conforming to the medial and lateral femoral posterior articular surfaces in the sagittal plane. In those studies, knee motion was analyzed via a series of images of various knee flexion angles taken under static conditions. (Hereafter, we will refer to this as the "stop-motion technique.")

Alternatively, in vivo three-dimensional (3D) knee motion studies have been performed since the 1990s using two-dimensional (2D) fluoroscopic images and several image registration techniques (e.g., image matching using a 2D image library, or 3D to 2D image registration), mainly for total knee arthroplasties [12–17]. In recent years, this technique has also been applied in studies of normal knee motion, utilizing contact points of the femur and tibia as evaluating parameters [18, 19]. Techniques employing these contact points are considered appropriate for examining contact conditions between femur and tibia and the movements of contact locations during knee motion [18, 19], which makes it possible to study the causes and the mechanisms of cartilage degeneration and injury in pathological knees [20], as well as the wear patterns of polyethylene inserts in total knee arthroplasty [15]. In such techniques, however, the positions of evaluation parameters (contact points) relative to femoral coordinates change with knee motion. In contrast, during techniques that employ anatomically defined axes or points, such as GCA or FFC, the positions of evaluation parameters relative to femoral coordinates do not change with knee motion. Therefore, such techniques are considered appropriate for assessing the relative motion between the femur and tibia, and especially when documenting the changes in relative position between the femoral and tibial condyles with knee motion in the medial and lateral compartments, respectively. However, no study to date has studied in vivo dynamic normal knee kinematics employing GCA or FFC as an evaluation parameter throughout the full range of motion. It is possible that the knee kinematics obtained under dynamic conditions may differ from those observed using stop-motion techniques due to the effects of acceleration and kinetic energy.

We hypothesized that normal knee kinematics obtained via in vivo dynamic motion analysis would yield different results from those previously reported using stop-motion techniques when knee kinematics are described by anatomically defined reference axes at the femoral condyles.

The purpose of this study was to analyze in vivo dynamic kinematics of the normal knee through the full range of motion via the 3D-to-2D registration technique, employing GCA as an evaluation parameter, and to compare the results with previous reports obtained using stop-motion techniques to evaluate this hypothesis.

## Materials and methods

We asked 20 healthy volunteers (10 male, 10 female) with no knee-related symptoms (pain, instability, click, locking, or limited range of motion), history of major trauma, or obvious deformity in the lower extremities to participate in this study. Mean age was 37.2 years (range 24–61 years). This study was performed according to the protocol approved by the Investigational Review Board of our institutions. All subjects provided informed consent to participate in this study.

The motion of the right knee was analyzed in all subjects. Computed tomography (CT) (SOMATOM® Sensation 16; Siemens, Munich, Germany) of the femur and tibia was obtained for each subject at 1 mm intervals. A 3D digital model of the femur and tibia was reconstructed from CT data using 3D visualization and modeling software (ZedView®; LEXI, Tokyo, Japan), and the anatomic coordinate systems were established by referencing several bony landmarks [21]. The tibial $z$-axis was defined as a line connecting the midpoint of the tibial eminence and the midpoint of the medial and lateral top of the talar dome. The tibial $y$-axis (positive anteriorly) was defined as a line drawn perpendicularly from the mediolateral center of the insertion of the posterior cruciate ligament to the $z$-axis. The tibial $x$-axis was defined as the cross product of the $z$-axis and $y$-axis. The $xy$ plane in this coordinate system was defined as the tibial axial plane. Using previously applied methods [1, 4, 5, 9], the medial and lateral posterior femoral condyles were approximated as spheres that best matched the geometries of the condyles. The GCA was defined as the segment connecting the centers of the spheres (Fig. 1). Knee motion was observed when subjects squatted from a standing position (knee fully extended to maximum flexion), and was recorded via a flat panel detector (AXIOM Artis® dTA; Siemens). All subjects stood with their feet in a comfortable rotation position (neutral rotation) [7].

The sampling frequency was 15 Hz, with an image area of 380 × 300 mm and resolution of 1240 × 960 pixels. The mean duration of one flexion of the knee was 8.4 s.

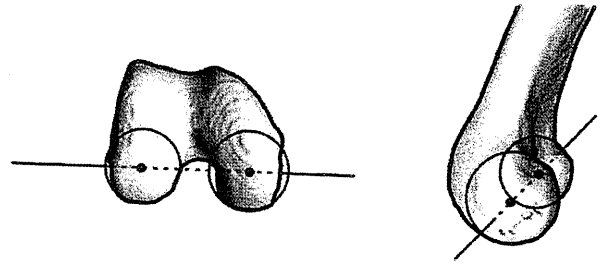

**Fig. 1** The geometric center axis is the line connecting the centers of spheres that represent the medial and lateral femoral posterior condyles

The mean angular velocity and sampling rate were 17.8°/s and 0.8 images/degree of knee flexion, respectively. The series of static lateral images were stored digitally. After the contours of the femur and tibia had been detected manually in these images, a 3D-to-2D technique using an automated shape-matching algorithm [21] was employed to determine the relative 3D positions of the femur and tibia in each fluoroscopic image (KneeMotion®; LEXI) (Fig. 2). By performing this procedure for all images, the relative motion between the femur and tibia could be obtained. The root mean square error (RMSE) was 0.3–0.8 mm for in-plane translation, 2.2 mm for out-of-plane translation, and 0.2–0.6° for rotation [22].

Relative motion between the femur and tibia was quantified as the movement of GCA projected onto the axial (*xy*) plane of the tibial coordinate system. The anteroposterior (AP) locations of the medial and lateral ends of all projected GCAs were evaluated as *y* values of the tibial coordinate system (Fig. 3). We determined the following parameters: (1) changes in the angle of the GCA on the tibial axial plane (rotation angle); (2) AP translations of the medial and lateral ends of the GCA; and (3) motion patterns in respective phases during knee flexion. Changes in the angle of the GCA on the tibial axial plane were calculated as the rotation angle around the *z*-axis (longitudinal axis) of the tibia, which is the relative axial rotation between the femoral and the tibial coordinate system based on the concept developed by Grood et al. [23]. The AP translations of the medial and lateral ends of the GCA were described using both absolute and normalized values. The absolute values were used for comparisons to previous reports, while the normalized values are reference data for evaluating motions of pathologic knees in other groups in the future. The absolute values of AP translations were normalized using the AP diameter of the proximal tibia (the distance from the most anterior point to the most posterior point of the *Y*-axis on the axial plane, which includes the tip of the fibula head). The midpoint of the AP diameter was defined as the 0% point, while the most anterior and posterior points were defined as the "anterior 100%" and "posterior 100%" points, respectively (Fig. 4). The AP translations of the medial and lateral ends of the GCA were described using "percent distances" by calculating the change in their "percent locations." The motion pattern was determined by observing AP translations of the medial and lateral ends of the GCA and also by capturing the locations of intersecting points of GCAs in respective phases according to the concepts of Asano et al. [1]. If both ends of the GCA showed posterior translations in the same phase, "bicondylar rollback motion" was considered to be present. Likewise, if only one end of the GCA showed AP translation and intersections of GCAs were observed in the contralateral compartment in the same phase, "lateral" or "medial pivot motion" was considered to be present. However, as a footnote, the term "rollback" is not a truly correct expression for explaining the trajectories of the GCA, because the GCA itself does not demonstrate rollback motion. Moreover, femoral condyles do not necessarily exhibit merely "rolling;" they can exhibit "sliding" as well. The condition of rolling requires that the zero velocity point is at the contact point between two surfaces, in this case the femur and tibia [24]. In addition, the term "pivot motion" may not be appropriate, as a specific motionless fulcrum does not exist. However, in this study, we used the terms "pivot motion" and "rollback" for the simple reason that they have been frequently used and are conceptually understood by clinicians.

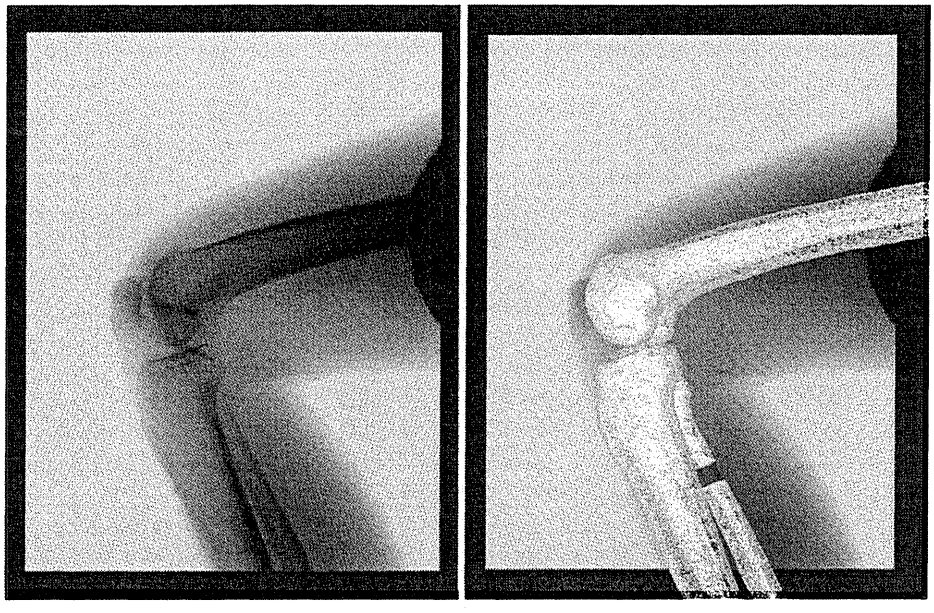

**Fig. 2** Example of the three-dimensional (3D) to two-dimensional (2D) registration technique. A 2D fluoroscopic image of the knee was downloaded and a 3D bone model was matched onto a 2D fluoroscopic image

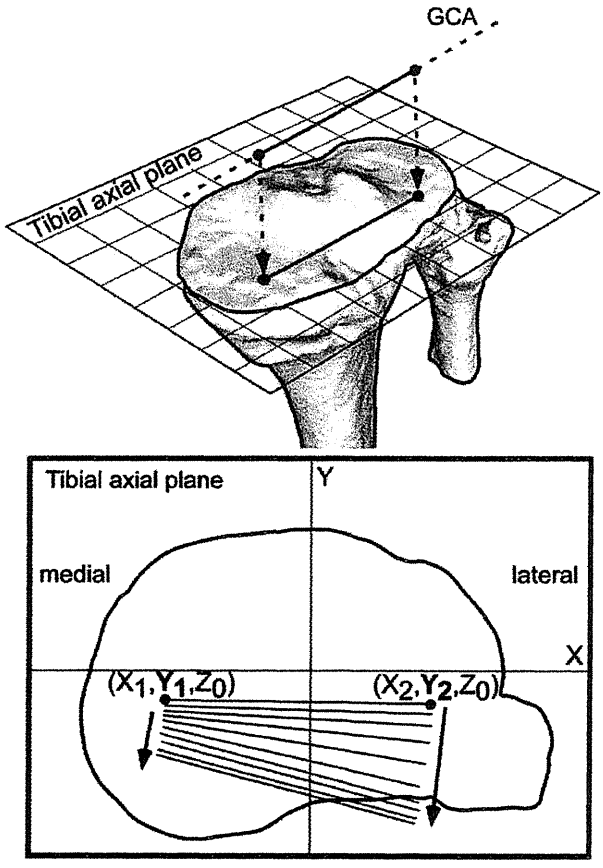


Fig. 3 Relative motion of the femur compared to the tibia. Movement of the GCA was projected onto the axial plane of the tibial coordinate system. Anteroposterior (AP) locations of the GCAs were evaluated as $y$ values of the tibial coordinate system

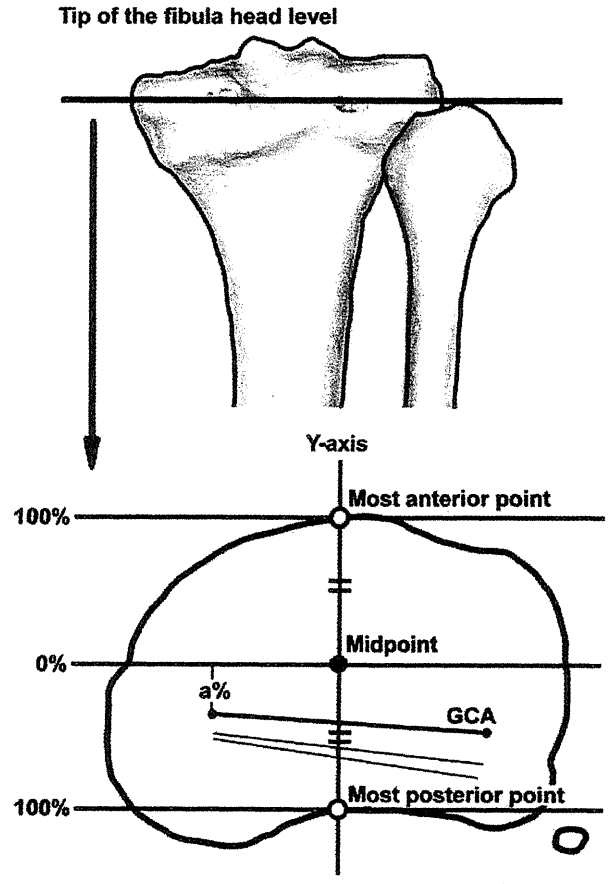


Fig. 4 The absolute values of AP translations were normalized. The AP translations of the medial and lateral ends of the GCA were described by percent distances obtained by calculating the change in the percent locations of them

To examine the reproducibility of knee motion patterns, changes to the angle of the GCA (rotation angle) and AP translations of the medial and lateral ends of the GCA, three subjects in this series were chosen for examination on two different days. At the time of the second examination, all subjects were asked to repeat the activities of the first examination while being recorded and examined using the same techniques. The intra-observer reproducibility of our parameters was then examined via an intra-class correlation coefficient (ICC). The mean and maximum differences in the rotation angle of GCA between the two examinations were 2° and 3°, respectively. The mean and maximum differences in total AP translation of the medial and lateral ends of the GCA were 1.6 and 2.7 mm (medial) and 1.7 and 2.8 mm (lateral), respectively. The ICC of the GCA rotation angle, the AP translation of the medial end of the GCA, and that of the lateral end of the GCA were 0.97, 0.74, and 0.87, respectively. All three knees displayed the same kinematics pattern in both examinations. The inter-observer errors were also examined. Two observers analyzed five subjects in this series. The mean and maximum differences in the rotation angle of GCA between the two examinations were 2.6° and 4°, respectively. The mean and maximum differences in the total AP translations of the medial and lateral ends of the GCA between two examinations were 0.8 and 2.7 mm (medial), and 1.1 and 2.7 mm (lateral), respectively. The ICC of the GCA rotation angle, the AP translation of the medial end of the GCA, and the AP translation of the lateral end of the GCA were 0.86, 0.81, and 0.98, respectively. In both examinations, relatively similar kinematic patterns were observed.

## Results

### Changes to the angle of the GCA on the tibial axial plane (rotation angle)

In all subjects, the GCA exhibited external rotation on the axial plane of the tibial coordinate system throughout knee flexion. This indicates that all subjects demonstrated

internal rotation of the tibia relative to the femur throughout knee flexion. The mean rotation angle was 26.1 ± 6.3° (range 11.8–40.3°, female 28.3 ± 6.1°, male 23.9 ± 6°).

### AP translations of the medial and lateral ends of the GCA

With regard to these parameters, values observed within the range of knee flexion angles (0–140°) that could be obtained by all subjects were employed for the calculations. Figures 5 and 6 show the AP translations of the medial and lateral ends of the GCA in the aforementioned range. The medial end of the GCA demonstrated anterior translation from 0° to nearly 100° flexion (mean translation 5.5 ± 3.7 mm, range 1.3 mm posterior to 12.2 mm anterior) and demonstrated posterior translation after nearly 100–140° (mean translation 3.9 ± 2.9 mm, range 2.7 mm anterior to 8.6 mm posterior), while the lateral end demonstrated consistent posterior translation throughout knee flexion (mean translation, 15.6 ± 5.0 mm, range 8.5–25.8 mm posterior) (Fig. 5). Using normalized values, the medial end of the GCA demonstrated anterior translation from 0° to nearly 100° flexion (mean translation 22.2 ± 15.1%, range 4.6% posterior to 46.6% anterior), and demonstrated posterior translation after nearly 100–140° (mean translation 14.9 ± 11.1%, range 11% anterior to 34.5% posterior), while the lateral end demonstrated consistent posterior translation throughout knee flexion (mean translation 60.4 ± 17.5%, range 32.3–93.5% posterior) (Fig. 6).

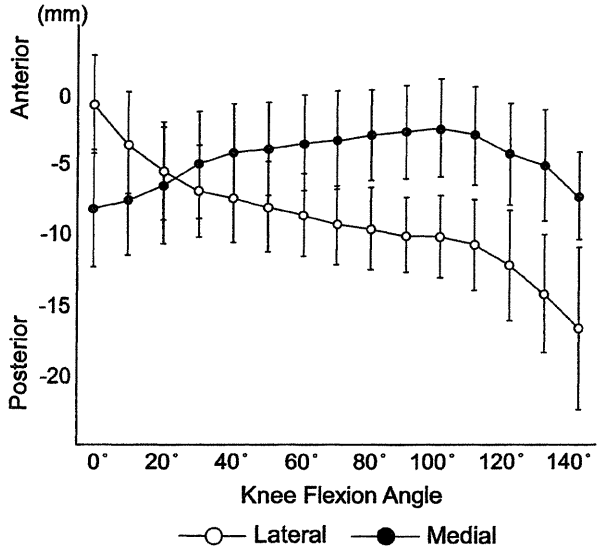


**Fig. 5** The absolute AP translation values for the medial and lateral ends of the GCA (mean ± SD)

### Motion patterns in respective phases during knee flexion

In all 20 knees, from full extension to nearly 120° flexion, intersecting points of GCAs were located in the medial compartment, while the lateral ends of GCAs showed posterior translations. This motion pattern was thought to represent so-called medial pivot motion. From nearly 120° flexion to full flexion, both medial and lateral ends of the GCA showed almost the same amount of posterior translation, representing so-called bicondylar rollback motion (Fig. 7). In 5 of 20 knees, lateral pivot motion was observed in the limited phase. That was caused by the anterior translation of the medial end of the GCA.

## Discussion

In this study, in vivo 3D dynamic kinematics of normal knees were evaluated through the full range of motion using the GCA for the first time. The results were then compared with those of previous studies employing stop-motion techniques.

In our study, the mean rotation angle of the GCA was 26.1°. Iwaki et al. [2] evaluated the stop-motion kinematics of cadaveric knees from full extension to 120° flexion by magnetic resonance imaging, utilizing the FFC as an evaluation parameter. In their study, the mean total rotation angle of the FFC was about 20° smaller than that of our study. Asano et al. [1] reported stop-motion kinematics in

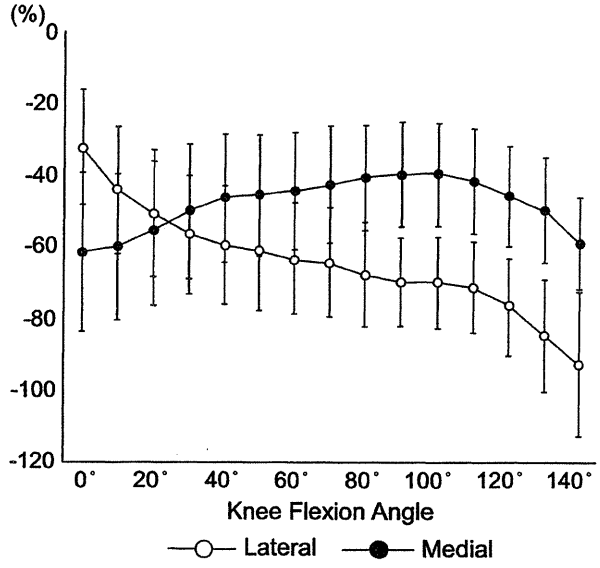


**Fig. 6** Normalized AP translation of the medial and lateral ends of the GCA (mean ± SD). The curves of the normalized AP translations were almost the same as those of the AP translations described by the absolute values shown in Fig. 5

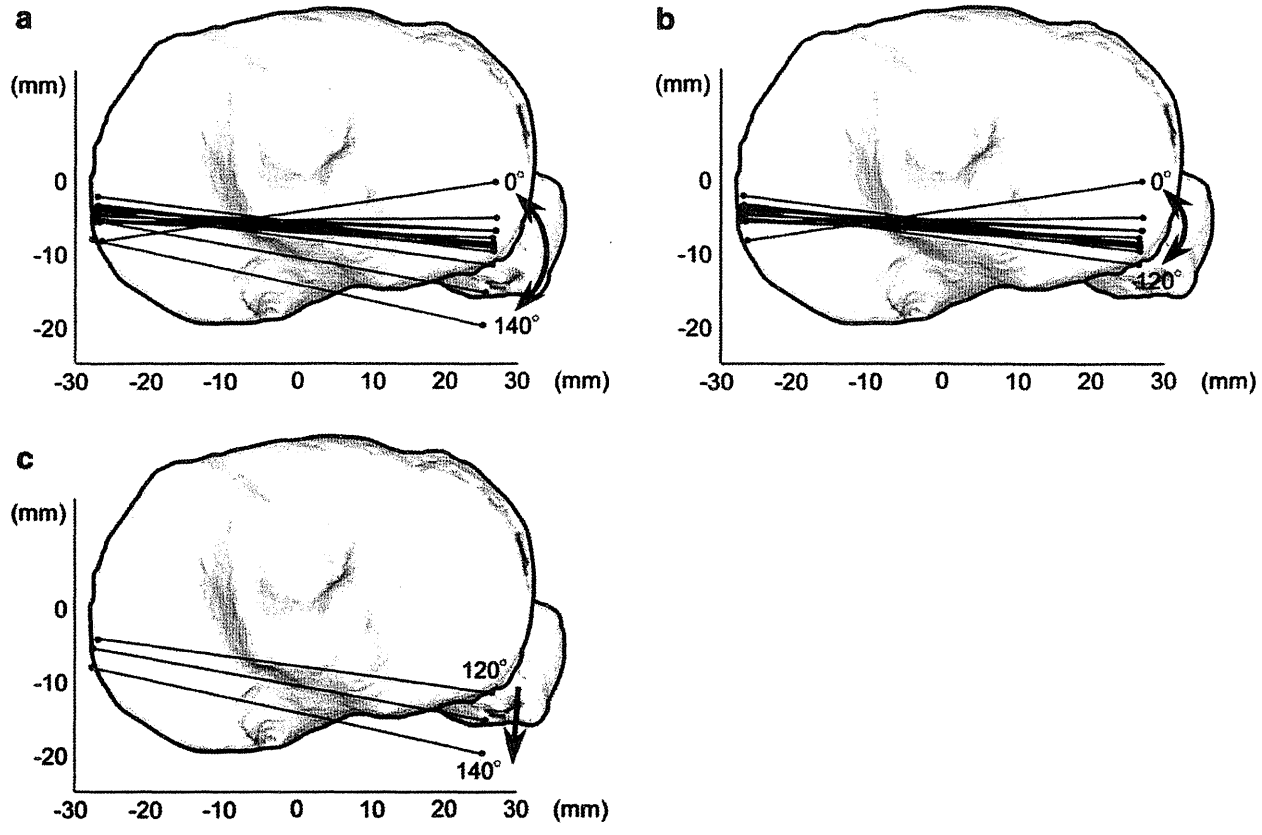


**Fig. 7** Appearance of projected GCAs on the tibial axial plane every 10° in one knee. **a** The typical pattern for the center of rotation in this series. **b** From full extension to 120° flexion. **c** From 120° flexion to full flexion

the range of 0–120° flexion of normal living knees under weight-bearing conditions using biplanar radiography, and described their kinematics using GCA measurement. According to that study, the mean total rotational angle of the GCA was 29.1°. These results were quite similar to our results in terms of rotation angle. Therefore, the mean rotational angle of GCA obtained by dynamic knee motion analysis did not differ greatly from that obtained by stop-motion techniques under in vivo conditions (Table 1).

Regarding the AP translations of the medial and lateral ends of the GCA, in our study, the medial end of the GCA demonstrated an anterior translation of 5.5 mm from full extension to nearly 100° flexion, followed by a posterior translation of 3.9 mm after nearly 100° to full flexion, while the lateral end demonstrated consistent posterior translation (15.6 mm) throughout knee flexion. This behavior of the medial and lateral ends of the GCA from full extension to 100° flexion was similar to that observed in previous in vivo stop-motion studies [1]. However, compared with the study of Iwaki et al. [2], although the lateral end of the GCA showed almost the same behavior, the medial end showed different behavior. The medial end of FFC stayed at almost the same point in Iwaki's study. The smaller axial rotation angle found in the cadaver study (as compared to our dynamic in vivo analysis) might have been caused by the absence of anterior translation of the medial end of the GCA. The difference in medial translation between the two studies was likely induced mainly by the use of living rather than cadaveric knees. Iwaki et al. [2] utilized cadaveric knees, so the effects of real-time changes in stresses applied to the knee by muscles and through weight-bearing on knee kinematics in the respective phases of knee flexion were absent. Actually, Hill et al. [7] reported the anterior translation of the medial femoral condyle in early to mid-flexion while evaluating living knee motion in normal subjects using the same methods and parameters. In our study, medial anterior translation may have occurred due to the effects of stresses applied to the knee via weight-bearing and muscle force while squatting.

In our study, all 20 knees demonstrated medial pivot motion from full extension to nearly 120° flexion. This motion pattern was also seen in previous studies [1, 2] from extension to nearly 120° flexion. Due to methodological limitations, these studies did not describe knee motion from nearly 120° to full flexion. However, Pinskerova et al. [3] recently reported on stop-motion knee kinematics in the

**Table 1** Comparison to previous stop motion studies that analyzed normal knees using the GCA

| | Subjects | Evaluation ROM (degrees) | Femorotibial axial rotation (degrees) | A-P translation (mm) medial | A-P translation (mm) lateral | Motion patterns of femur |
|---|---|---|---|---|---|---|
| Asano et al [1] | 6 in vivo knees | 0 to 120 | 29.1 ER | 5.0 AT(to 105°) 1.2 PT(from 105°) | 17.8 PT | MP |
| [2]+ [3] | | -5 to 160 | Less than 20.0 ER | 10.0 PT | 24.0 PT | MP(to 120°) BR(from 120°) |
| Iwaki et al [2] | 6 cadaver knees | -5 to 120 | 20.0 ER | 2.0 PT | 19.0 PT | MP |
| Pinskerova et al [3] | 4 cadaver knees | 120 to 160 | Slight IR | 8.0 PT | 5.0 PT | BR |
| This study | 20 in vivo knees | full extension to full flexion | 26.1 ER | 5.5 AT(to 100°) 3.9 PT(from 100°) | 15.6 PT | MP(to 120°) BR(from 120°) |

ER=external rotation; IR=internal rotation; AT=anterior translation; PT=posterior translation; MP=medial pivot; BR=bicondylar rollback;

range of 120–160° flexion utilizing cadaveric knees, employing the FFC as an evaluation parameter. In their study, the tibiofemoral movement from 120 to 160° was characterized following Iwaki et al. [2]. They showed that the FFC at the medial and lateral femoral condyles moved back by 8 and 5 mm, respectively, displaying bicondylar rollback motion. In this study, although the amount of femoral posterior translation of the medial and lateral compartments was slightly different from that of Pinskerova's study, femoral bicondylar rollback motion was also observed during dynamic knee motion from 120° to maximum flexion (Table 1), indicating that the motion pattern observed in the deep flexion range during the stop-motion technique was also reproduced by dynamic knee motion analysis. The difference in the amount of femoral posterior translation of the medial and lateral compartments between stop-motion and dynamic motion analysis could have been induced by the aforementioned difference between in vivo and cadaveric subjects.

As a result of this study, the previously reported normal knee kinematics obtained via stop-motion techniques were also reproduced using dynamic knee motion analysis in living knees in terms of axial rotation, AP translation of medial and lateral femoral condyles, and motion pattern, indicating that our hypothesis was not confirmed. As reported, our dynamic knee kinematics did not differ greatly from those obtained through stop-motion techniques. Although the specific reasons for this similarity are unknown, we can speculate that there are several causes. First, because the subjects recruited in this study were asked to squat relatively slowly during the measurement of knee motion, the kinematics may not have been affected as strongly compared to the acceleration or kinetic energy seen during normal dynamic motion. Therefore, it is possible that knee kinematics within the same activity but performed at a higher velocity (or other activities such as walking or stair climbing) would result in outcomes different from that of stop motion. Second, as normal knees were analyzed in this study, the functions of knee ligaments such as the anterior and posterior cruciate ligaments were intact. Therefore, it is thought that those healthy ligaments enabled stable knee kinematics [25], especially during relatively slow activity, resulting in kinematics similar to those found in stop-motion techniques. Hence, although there might be differences between the static and dynamic conditions in terms of kinetics (including loads applied to ligaments and joint surfaces), kinematic parameters related to the relative positions of the femur and tibia did not differ greatly between the two methods under the conditions of this study. It is possible that knees with decreased ligament function

due to such conditions as anterior cruciate deficiency or osteoarthritis may demonstrate different kinematics from those seen in stop-motion analysis.

Our study had several limitations. First, the image registration technique using single-plane fluoroscopy shows limited out-of-plane accuracy. This reduced accuracy might affect the determination of the relative position between the femur and tibia [22]. Second, as described above, only squat (flexion) motion was analyzed in this study. Although this activity was thought to be adequate for evaluating knee motion in the full range of motion under weight-bearing conditions, other dynamic and daily activities such as walking, stair climbing, or kneeling should also be examined to obtain more clinically important reference data.

In summary, our investigation demonstrated some differences from previous studies in terms of anterior translation of the medial femoral condyle, resulting in a minor disparity in the rotational angle of the GCA. However, in general, the results obtained by our dynamic motion analysis were very similar to those obtained by previous stop-motion techniques when knee motion was described by GCA. This is especially true when comparing the results obtained under in vivo weight-bearing conditions in previous studies for the rotation angle, AP translation, and motion patterns. Therefore, the authors believe that the results obtained in this dynamic knee motion study support previously reported results obtained using stop-motion techniques. However, further studies are thought to be necessary, as it is possible that the dynamic knee kinematics are not necessarily similar to the kinematics obtained by stop-motion techniques when the type of activity or the velocity of the activity differs from that used in this study, and also when pathological subjects such as unstable knees are observed.

Observing knee motion under in vivo conditions with all the factors that influence living subjects is crucial to obtaining clinically important data. Furthermore, our results should provide useful control data for dynamic kinematic analyses of pathologic knees in the future.

**Acknowledgments** The authors would like to thank the entire staff of the Department of Radiology of the Niigata University Medical and Dental Hospital for their technical support and cooperation.

**Conflict of interest** The authors did not receive and will not receive any benefits or funding from any commercial party related directly or indirectly to the subject of this article.

## References

1. Asano T, Akagi M, Tanaka K, Tamura J, Nakamura T. In vivo three-dimensional knee kinematics using a biplanar image-matching technique. Clin Orthop Relat Res. 2001;388:157–66.
2. Iwaki H, Pinskerova V, Freeman MA. Tibiofemoral movement 1: the shapes and relative movements of the femur and tibia in the unloaded cadaver knee. J Bone Joint Surg Br. 2000;82:1189–95.
3. Pinskerova V, Samuelson KM, Stammers J, Maruthainar K, Sosna A, Freeman MA. The knee in full flexion. J Bone Joint Surg Br. 2009;91:830–4.
4. Kurosawa H, Walker PS, Abe S, Garg A, Hunter T. Geometry and motion of the knee for implant and orthotic design. J Biomech. 1985;18:487–99.
5. Walker PS, Kurosawa H, Rovick JS, Zimmerman RA. External knee joint design based on normal motion. J Rehabil Res Dev. 1985;22:9–22.
6. Churchill DL, Incavo SJ, Johnson CC, Beynnon BD. The transepicondylar axis approximates the optimal flexion axis of the knee. Clin Orthop Relat Res. 1998;356:111–8.
7. Hill PF, Vedi V, Williams A, Iwaki H, Pinskerova V, Freeman MA. Tibiofemoral movement 2: the loaded and unloaded living knee studied by MRI. J Bone Joint Surg Br. 2000;82:1196–8.
8. Nakagawa S, Kadoya Y, Todo S, Kobayashi A, Sakamoto H, Freeman MA, Yamano Y. Tibiofemoral movement 3: full flexion in the living knee studied by MRI. J Bone Joint Surg Br. 2000; 82:1199–200.
9. Most E, Axe J, Rubash H, Li G. Sensitivity of the knee joint kinematics calculation to selection of flexion axes. J Biomech. 2004;37:1743–8.
10. Williams A, Logan M. Understanding tibio-femoral motion. Knee. 2004;11:81–8.
11. Asano T, Akagi M, Nakamura T. The functional flexion-extension axis of the knee corresponds to the surgical epicondylar axis: in vivo analysis using a biplanar image matching technique. J Arthroplasty. 2005;20:1060–7.
12. Banks SA, Markovich GD, Hodge WA. In vivo kinematics of cruciate-retaining and -substituting knee arthroplasties. J Arthroplasty. 1997;12:297–304.
13. Hoff WA, Komistek RD, Dennis DA, Gabriel SM, Walker SA. Three-dimensional determination of femoral-tibial contact positions under in vivo conditions using fluoroscopy. Clin Biomech. 1998;13:455–72.
14. Yamazaki T, Watanabe T, Nakajima Y, Sugamoto K, Tomita T, Yoshikawa H, Tamura S. Improvement of depth position in 2-D/3-D registration of knee implants using single-plane fluoroscopy. IEEE Trans Med Imaging. 2004;23:602–12.
15. Li G, Suggs J, Hanson G, Durbhakula S, Johnson T, Freiberg A. Three-dimensional tibiofemoral articular contact kinematics of a cruciate-retaining total knee arthroplasty. J Bone Joint Surg Am. 2006;88:395–402.
16. Komistek RD, Mahfouz MR, Bertin KC, Rosenberg A, Kennedy W. In vivo determination of total knee arthroplasty kinematics. J Arthroplasty. 2008;23:41–50.
17. Tamaki M, Tomita T, Yamazaki T, Hozack WJ, Yoshikawa H, Sugamoto K. In vivo kinematic analysis of a high-flexion posterior stabilized fixed-bearing knee prosthesis in deep knee-bending motion. J Arthroplasty. 2008;23:879–85.
18. Komistek RD, Dennis DA, Mahfouz M. In vivo fluoroscopic analysis of the normal human knee. Clin Orthop Relat Res. 2003;410:69–81.
19. Moro-oka T, Hamai S, Miura H, Shimoto T, Higaki H, Fregly BJ, Iwamoto Y, Banks SA. Dynamic activity dependence of in vivo normal knee kinematics. J Orthop Res. 2008;26:428–34.
20. Li G, Moses JM, Papannagari R, Pathare NP, DeFrate LE, Gill TJ. Anterior cruciate ligament deficiency alters the in vivo motion of the tibiofemoral cartilage contact points in both the anteroposterior and mediolateral directions. J Bone Joint Surg Am. 2006;88:1826–34.
21. Sato T, Koga Y, Omori G. Three-dimensional lower extremity alignment assessment system. J Arthroplasty. 2004;19:620–8.

22. Kobayashi K, Tanaka N, Odagawa K, Sakamoto M, Tanabe Y. Image-based matching for natural knee kinematics measurement using single-plane fluoroscopy. J Jpn Soc Exp Mech. 2009;9: 162–6.
23. Grood ES, Suntay WJ. A joint coordinate system for the clinical description of three-dimensional motions: application to the knee. J Biomech Eng. 1983;105:136–44.
24. Blaha JD, Mancinelli CA, Simons WH, Kish VL, Thyagarajan G. Kinematics of the human knee using an open chain cadaver model. Clin Orthop Relat Res. 2003;410:25–34.
25. Dennis DA, Mahfouz MR, Komistek RD, Hoff W. In vivo determination of normal and anterior cruciate ligament-deficient knee kinematics. J Biomech. 2005;38:241–53.